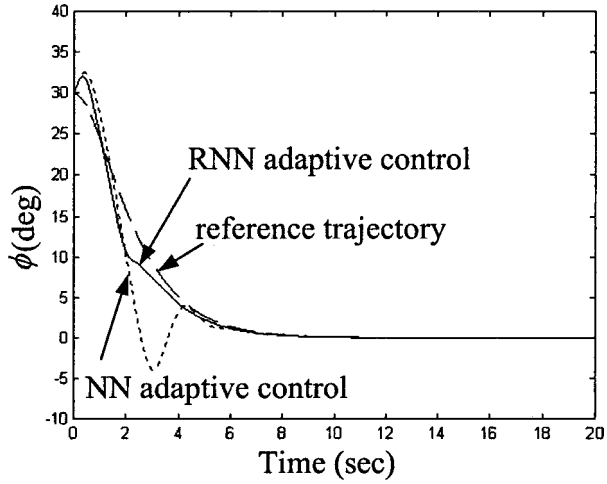

a) State responses

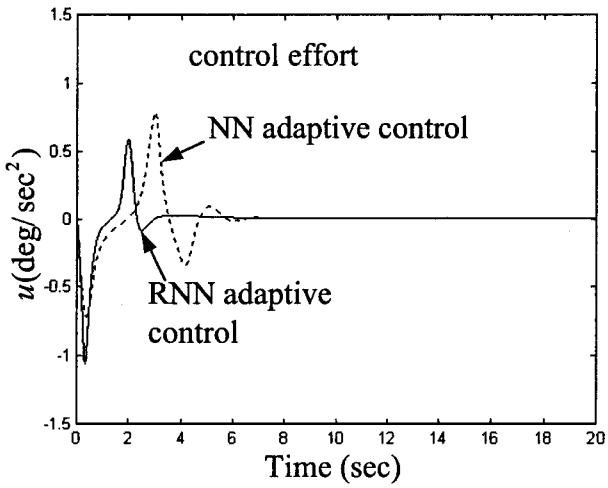

b) Associated control efforts

Fig. 1 NN and RNN adaptive control responses of wing-rock motion.

become more unstable for the parameter convergence. In the following, a comparison of the tracking accuracy is presented by using the NN adaptive controller in Ref. 4 and the proposed RNN adaptive controller. The NN adaptive controller used a traditional radial basis function with fixed center and width. The proposed RNN adaptive controller uses a radial basis function with an internal feedback loop and tunes the center, width, and feedback gain of the radial basis function. Simulations of the NN and RNN adaptive control systems with five hidden layer neurons for the initial condition ($\phi = 30$ deg and $\dot{\phi} = 10$ deg/s) is shown in Fig. 1. The state responses are shown in Fig. 1a, and the associated control efforts are shown in Fig. 1b. Simulation results show that the tracking performance is considerably improved by using the proposed RNN adaptive control system.

V. Conclusions

In this Note, an RNN adaptive control system is proposed to control a wing-rock motion system. This Note has successfully demonstrated that the adaptive technique has been applied for the design of an RNN system. This RNN adaptive controller can be applied to a completely unknown system dynamic function. The adaptive laws based on the Lyapunov stability theorem can automatically adjust the interconnection weights of the RNN. Thus, the stability of the developed RNN adaptive control system can be guaranteed. Simulation results have demonstrated that the proposed RNN adaptive controller can achieve favorable control performance for the wing-rock motion system.

Acknowledgments

This work was supported by the National Science Council (NSC) of the Republic of China under Grant NSC 90-2213-E-155-016. The authors are grateful to the reviewers and to the Associate Editor for their valuable comments.

References

[1] Konstadinopoulos, P., Mook, D. T., and Nayfeh, A. H., "Subsonic Wing Rock of Slender Delta Wings," *Journal of Aircraft*, Vol. 22, No. 3, 1985, pp. 223–228.

[2] Elzebda, J. M., Nayfeh, A. H., and Mook, D. T., "Development of an Analytical Model of Wing Rock for Slender Delta Wings," *Journal of Aircraft*, Vol. 26, No. 8, 1989, pp. 737–743.

[3] Nayfeh, A. H., Elzebda, J. M., and Mook, D. T., "Analytical Study of the Subsonic Wing-Rock Phenomenon for Slender Delta Wings," *Journal of Aircraft*, Vol. 26, No. 9, 1989, pp. 805–809.

[4] Singh, S. N., Yim, W., and Wells, W. R., "Direct Adaptive and Neural Control of Wing-Rock Motion of Slender Delta Wings," *Journal of Guidance, Control, and Dynamics*, Vol. 18, No. 1, 1995, pp. 25–30.

[5] Monahemi, M. M., and Krstic, M., "Control of Wing-Rock Motion Using Adaptive Feedback Linearization," *Journal of Guidance, Control, and Dynamics*, Vol. 19, No. 4, 1996, pp. 905–912.

[6] Lee, C. H., and Teng, C. C., "Indentification and Control of Dynamic Systems Using Recurrent Fuzzy Neural Networks," *IEEE Transactions on Fuzzy Systems*, Vol. 8, No. 4, 2000, pp. 349–366.

[7] Wang, L. X., *Adaptive Fuzzy Systems and Control—Design and Stability Analysis*, Prentice–Hall, Englewood Cliffs, NJ, 1994, pp. 140–154.

Angular Velocity Determination Directly from Star Tracker Measurements

John L. Crassidis*
University at Buffalo, State University of New York, Amherst, New York 14260-4400

Introduction

STAR trackers are increasingly used on modern day spacecraft. With the rapid advancement of imaging hardware and high-speed computer processors, current trackers are small and routinely achieve arc-second attitude accuracy.[1] Typical sampling rates for these trackers range from 1 to 10 Hz. As computer processor technology advances, these frequencies will increase, leading to filter designs that provide even more accurate results.

The body angular velocity can be derived using a derivative approach in the attitude kinematics model. For example, if the attitude quaternion $\boldsymbol{q}$ and its derivative $\dot{\boldsymbol{q}}$ (which is usually approximated by a finite difference of the attitude) are known then the angular velocity $\boldsymbol{\omega}$ can be computed from the kinematics equation, with $\boldsymbol{\omega} = 2\Xi^T(\boldsymbol{q})\dot{\boldsymbol{q}}$, where $\Xi(\boldsymbol{q})$ is a 4×3 matrix function of the quaternion (see Ref. 2 for more details). However, this approach requires knowledge of the attitude, which is determined from the star reference and body measurement vectors. In this Note a new and simple approach to determine the angular velocity is shown that depends only on knowledge of the body vector measurements, which are obtained directly from the star tracker. Therefore, angular velocities can still be determined in the event of star pattern recognition anomalies. Also, these velocities can be used to control the spacecraft in the event of gyro failures.

Angular Velocity Determination

In this section a least-squares approach is used to determine the angular velocity from star tracker body measurements

Received 10 December 2001; revision received 31 May 2002; accepted for publication 25 June 2002.

*Associate Professor, Department of Mechanical and Aerospace Engineering. Senior Member AIAA.

alone. Consider the following unit-vector measurement model at time t_k:

$$\tilde{\boldsymbol{b}}_i(k) = A(k)\boldsymbol{r}_i + \boldsymbol{v}_i(k) \tag{1}$$

where $\tilde{\boldsymbol{b}}_i(k)$ is the ith body measurement vector, $A(k)$ is the proper-orthogonal attitude matrix, $\boldsymbol{r}_i$ is the star reference vector, and $\boldsymbol{v}_i(k)$ is the measurement noise that is given by a zero-mean Gaussian white-noise process. Shuster[3] has shown an analysis of the probability density function for the measurement error involving unit-vector observations. A significant conclusion is that from a practical standpoint the probability density on the sphere is indistinguishable from the corresponding density on the tangent plane, so that the unit vector can in fact be used in standard forms with $\sigma_i^2 I_{3\times 3}$, where $I_{3\times 3}$ is a 3×3 identity matrix, as the measurement noise covariance. Also, we note that the inertially fixed star reference vector $\boldsymbol{r}_i$ is time-independent, neglecting effects such as proper motion and velocity aberration.

Taking the difference between successive measurements of Eq. (1) gives

$$\tilde{\boldsymbol{b}}_i(k+1) - \tilde{\boldsymbol{b}}_i(k) = [A(k+1) - A(k)]\boldsymbol{r}_i + \boldsymbol{v}_i(k+1) - \boldsymbol{v}_i(k) \tag{2}$$

We assume that the body angular velocity $\boldsymbol{\omega}$ is constant between t_k and t_{k+1} and ignore terms higher than first order in $\boldsymbol{\omega}\Delta t$, where $\Delta t \equiv t_{k+1} - t_k$ is the sampling interval. With these assumptions the following first-order approximation can be used[2]:

$$A(k+1) \approx \{I - \Delta t[\boldsymbol{\omega}(k)\times]\}A(k) \tag{3}$$

where $[\boldsymbol{\omega}(k)\times]$ is the cross-product matrix, given by

$$[\boldsymbol{\omega}(k)\times] = \begin{bmatrix} 0 & -\omega_3(k) & \omega_2(k) \\ \omega_3(k) & 0 & -\omega_1(k) \\ -\omega_2(k) & \omega_1(k) & 0 \end{bmatrix} \tag{4}$$

Substituting Eq. (3) into Eq. (2) gives

$$\tilde{\boldsymbol{b}}_i(k+1) - \tilde{\boldsymbol{b}}_i(k) = -\Delta t[\boldsymbol{\omega}(k)\times]A(k)\boldsymbol{r}_i + \boldsymbol{v}_i(k+1) - \boldsymbol{v}_i(k) \tag{5}$$

Our goal is to determine an angular velocity estimate independent of attitude and the reference vectors. This is accomplished by solving Eq. (1) in terms of $A(k)\boldsymbol{r}_i$ and substituting the resultant into Eq. (5), which yields

$$(1/\Delta t)[\tilde{\boldsymbol{b}}_i(k+1) - \tilde{\boldsymbol{b}}_i(k)] = [\tilde{\boldsymbol{b}}_i(k)\times]\boldsymbol{\omega}(k) + \boldsymbol{w}_i(k) \tag{6}$$

where $\boldsymbol{w}_i(k)$ is the new effective measurement noise vector given by

$$\boldsymbol{w}_i(k) \equiv [\boldsymbol{\omega}(k)\times]\boldsymbol{v}_i(k) + (1/\Delta t)[\boldsymbol{v}_i(k+1) - \boldsymbol{v}_i(k)] \tag{7}$$

Note that Δt will have finite values because discrete-time measurements are assumed.

The new measurement noise $\boldsymbol{w}_i(k)$ in Eq. (6) is now a function of the angular velocity vector. Assuming a stationary noise process for $\boldsymbol{v}_i$, the following covariance expression can be derived:

$$E\left\{\boldsymbol{w}_i(k)\boldsymbol{w}_i^T(k)\right\} = \sigma_i^2[\boldsymbol{\omega}(k)\times][\boldsymbol{\omega}(k)\times]^T + \left(2\sigma_i^2/\Delta t^2\right)I_{3\times 3} \tag{8}$$

where $E\{\ \}$ denotes expectation. If the bandwidth of the attitude variations (that is, the frequency content) is well below the Nyquist frequency with a safety factor of 10, then $\|\boldsymbol{\omega}(k)\|\Delta t < \pi/10$ for all k. This condition obviously holds when the spacecraft is rotating slowly compared to the sampling rate, which is required by the assumptions made leading to Eq. (6). Because the 2-norm gives $\|[\boldsymbol{\omega}(k)\times]\| = \|\boldsymbol{\omega}(k)\|$, then the following inequality is true:

$$\left\|\sigma_i^2[\boldsymbol{\omega}(k)\times][\boldsymbol{\omega}(k)\times]^T\right\| < \frac{\pi^2}{100}\frac{\sigma_i^2}{\Delta t^2} \ll \frac{2\sigma_i^2}{\Delta t^2} \tag{9}$$

Using Eq. (9), then the last term in Eq. (8) dominates the first term on the right-hand side, which can effectively be ignored.

Equation (6) can now be cast into a linear least-squares form for all measurement vectors, which leads to

$$\hat{\boldsymbol{\omega}}(k) = \frac{1}{\Delta t}\left\{\sum_{i=1}^{n}\bar{\sigma}_i^{-2}[\tilde{\boldsymbol{b}}_i(k)\times]^T[\tilde{\boldsymbol{b}}_i(k)\times]\right\}^{-1} \times \sum_{i=1}^{n}\bar{\sigma}_i^{-2}[\tilde{\boldsymbol{b}}_i(k)\times]^T\tilde{\boldsymbol{b}}_i(k+1) \tag{10}$$

where $\hat{\boldsymbol{\omega}}(k)$ is the estimate of $\boldsymbol{\omega}(k)$ and $\bar{\sigma}_i^2 \equiv 2\sigma_i^2/\Delta t^2$ is the effective measurement error variance. Only knowledge of the body vector measurements, sampling interval, and measurement covariance are required to derive an angular velocity estimate. Therefore, the attitude and star reference vectors are not required to be known. Hence, stars do not need to be identified to determine the angular velocity. However, knowledge of the same star measurement $\tilde{\boldsymbol{b}}_i$ at times t_{k+1} and t_k is required to estimate $\boldsymbol{\omega}$ at time t_k. This time delay is an unfortunate result of the finite difference, but becomes less significant as the sampling interval decreases. This condition still exists when a finite difference approach is used from a kinematics model with a known attitude to estimate the angular velocity.

We now derive the estimate error covariance. Multiplying both sides of Eq. (6) by Δt and substituting the resultant for $\tilde{\boldsymbol{b}}_i(k+1)$ into Eq. (10) leads to

$$\hat{\boldsymbol{\omega}}(k) - \boldsymbol{\omega}(k) = \left\{\sum_{i=1}^{n}\bar{\sigma}_i^{-2}[\tilde{\boldsymbol{b}}_i(k)\times]^T[\tilde{\boldsymbol{b}}_i(k)\times]\right\}^{-1} \times \sum_{i=1}^{n}\bar{\sigma}_i^{-2}[\tilde{\boldsymbol{b}}_i(k)\times]^T\boldsymbol{w}_i(k) \tag{11}$$

Equation (11) involves the measurements $\tilde{\boldsymbol{b}}_i(k)$ themselves. The actual covariance should be computed by replacing $\tilde{\boldsymbol{b}}_i(k)$ with $A(k)\boldsymbol{r}_i + \boldsymbol{v}_i(k)$ from Eq. (1). However, using a similar analysis as the one shown in Ref. 3 indicates that the errors produced by ignoring this replacement are higher order in nature and thus are negligible. Therefore, the predicted error covariance (that is, the best available estimate of the error covariance) is simply given by

$$P(k) \equiv E\{[\hat{\boldsymbol{\omega}}(k) - \boldsymbol{\omega}(k)][\hat{\boldsymbol{\omega}}(k) - \boldsymbol{\omega}(k)]^T\} \approx \left\{\sum_{i=1}^{n}\bar{\sigma}_i^{-2}[\tilde{\boldsymbol{b}}_i(k)\times]^T[\tilde{\boldsymbol{b}}_i(k)\times]\right\}^{-1} \tag{12}$$

At least two noncollinear body vectors are required for observability [that is, for the inverse in Eq. (12) to exist]. The error covariance still depends on the sampling interval from $\bar{\sigma}_i^2$. Also, if $\bar{\sigma}_i^2$ is replaced by σ_i^2 this yields the attitude error covariance, which can be derived from maximum likelihood.[3] This shows an interesting similarity between the angular velocity estimation algorithm presented here and standard attitude determination algorithms.

Equation (10) is based upon a first-order difference approximation. This approach is accurate only when Eq. (3) is a valid approximation. Other approximations can be used, which might give better accuracies for high angular velocities (that is, when the bandwidth of the attitude variations is near the Nyquist frequency). However, some of these approximations might actually give worse results than the first-order difference approximation for motions well below the Nyquist frequency (as will be shown). Two other approximations will be considered here: a central difference approximation and a second-order difference approximation.[4] The derivation for each is similar to the first-order difference approximation, and so for brevity these derivations are omitted.

Using a central difference, the angular velocity estimate can be shown to be given by

$$\hat{\boldsymbol{\omega}}(k) = \frac{1}{2\Delta t}\left\{\sum_{i=1}^{n}\bar{\sigma}_i^{-2}[\tilde{\boldsymbol{b}}_i(k)\times]^T[\tilde{\boldsymbol{b}}_i(k)\times]\right\}^{-1} \times \sum_{i=1}^{n}\bar{\sigma}_i^{-2}[\tilde{\boldsymbol{b}}_i(k)\times]^T[\tilde{\boldsymbol{b}}_i(k+1) - \tilde{\boldsymbol{b}}_i(k-1)] \tag{13}$$

where $\bar{\sigma}_i^2 \equiv \sigma_i^2/\Delta t^2$. The error-covariance derivation leads to the same expression given in Eq. (12) with $\bar{\sigma}_i^2 = (1/\Delta t^2)\sigma_i^2$. Using a second-order difference, the angular velocity estimate can be shown to be given by

$$\hat{\omega}(k) = \frac{1}{2\Delta t}\left\{\sum_{i=1}^{n} \bar{\sigma}_i^{-2}[\tilde{\boldsymbol{b}}_i(k)\times]^T[\tilde{\boldsymbol{b}}_i(k)\times]\right\}^{-1} \times \sum_{i=1}^{n} \bar{\sigma}_i^{-2}[\tilde{\boldsymbol{b}}_i(k)\times]^T[4\tilde{\boldsymbol{b}}_i(k+1) - \tilde{\boldsymbol{b}}_i(k+2)] \tag{14}$$

where $\bar{\sigma}_i^2 \equiv [(13\sigma_i^2)/(2\Delta t^2)]$ is the measurement error covariance. The error-covariance derivation leads to the same expression given in Eq. (12) with $\bar{\sigma}_i^2 = [13/(2\Delta t^2)]\sigma_i^2$.

The central difference approach gives a lower standard deviation in the estimate noise (by a factor of $\sqrt{2}/2$) than the first-order difference approach; however, the central difference requires storage of $\tilde{\boldsymbol{b}}_i$ at times t_k and t_{k-1}, which increases the computational burden (especially when tracking the stars). The second-order algorithm provides a higher-order approximation, compared to the first-order approach, which might lead to more accurate results for higher body angular velocities (that is, the estimate errors might remain within their respective 3-σ bounds). But this comes at the price of an increased standard deviation in the estimate noise (by a factor of $\sqrt{13}/2$). Also, the second-order algorithm requires two time steps ahead to estimate the angular velocity at the current time. The first-order algorithm requires only one time step ahead. For these reasons this algorithm should be used when possible, under the Nyquist limit assumption.

It is imperative that the angular estimate calculations using Eqs. (10), (13), or (14) be done with the same star reference at different sampling periods because the reference vector is assumed to be constant. Care must be given to the available stars, keeping track of ones that enter or leave the field of view (FOV). If a star leaves the FOV at time t_{k+1}, then this star should not be used to compute the finite difference. This can be easily employed using simple tracking logic, such as computing inner star angles between successive body measurements (see Ref. 5 for details).

Simulation Example

Simulation results are shown using a two-star tracker configuration with actual star reference vectors to determine the angular velocity of a rotating spacecraft in a low Earth equatorial orbit. Each star tracker is assumed to sense up to 10 stars in an 8×8 deg FOV. The catalog contains stars that can be sensed up to a magnitude of 6.0 (larger magnitudes indicate dimmer stars). The spacecraft is assumed to be nearly Earth pointing with a body angular velocity rotation given by

$$\omega(t) = [0.0001\sin(0.01t) \quad 0.0011 \quad 0.0001\cos(0.01t)]^T \text{ rad/s} \tag{15}$$

Each star tracker is pointed away from the Earth with one star tracker pointed 45 deg in the north direction and the other is pointed 45 deg in the south direction. Therefore, the star tracker boresights are 90 deg apart. The sampling interval for each tracker is given by $\Delta t = 0.1$ s. Also, a standard deviation of $0.001\pi/180$ rad has been used to generate each synthetic body measurement set.

A plot of the available stars from both trackers over a 40-min simulation is shown in Fig. 1. The minimum number of available stars is 9 with a maximum of 20. In general, as the number of available stars decreases the estimation accuracy degrades, although this also depends on the angle separation between stars. For the simulation run the first-order difference has been used to determine the angular velocity, given by Eq. (10). A plot of the X-axis errors, with 3-σ bounds computed from Eq. (12), is shown in Fig. 2. Clearly, the computed 3-σ boundaries do indeed bound the estimation errors. Also, as the number of available stars decreases the 3-σ bounds and actual errors increase as expected. The computed angular velocities at each time are given by the top plot of Fig. 3. These velocities are filtered using a simple α filter,[6] with a gain

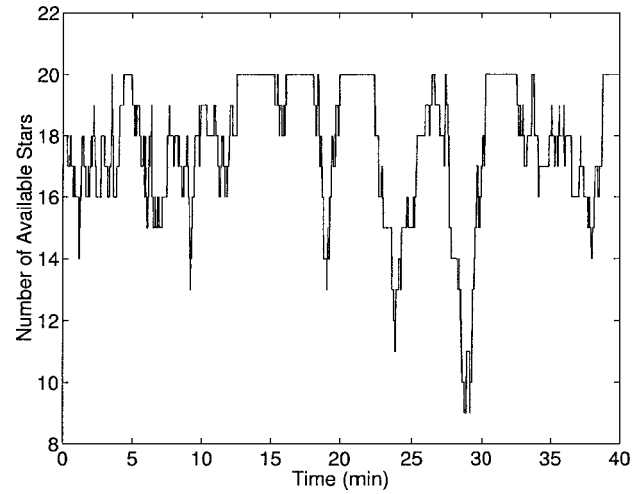

Fig. 1 Number of available stars.

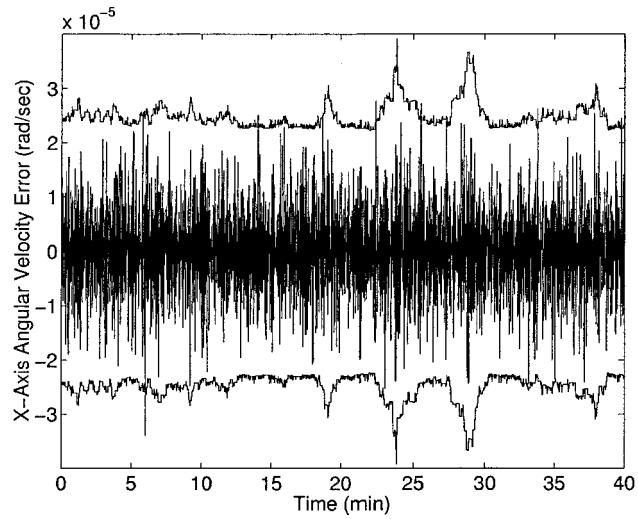

Fig. 2 X axis error with 3-σ bounds.

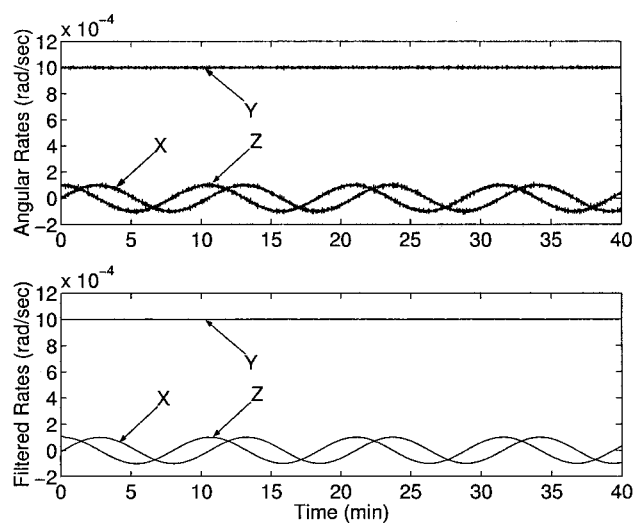

Fig. 3 Computed and filtered angular velocities.

set to $\alpha = 0.1$. The results are shown by the bottom plot of Fig. 3. This simple filter increases the accuracy by an order of magnitude without adding significant delay into the system. Furthermore, as the sampling frequency increases, through judicious filtering these star-tracker-derived velocities might eventually compete with the accuracy of modern day gyros. For this simulation, when the sampling frequency is given by 500 Hz the filtered velocities achieve an accuracy of about 0.05 μrad/s.

Conclusions

In this Note a new approach was shown to determine the angular velocity vector directly from star tracker measurements. The main advantage of this approach is that it requires no information of the star reference vectors or the attitude. Algorithms based on various difference approximations were developed. The estimate error covariances for each approximation have also been shown. Each approximation requires a time delay in the angular velocity estimate, which becomes less significant as the sampling interval decreases. Simulations results used a realistic star tracker configuration. Results indicated that very accurate angular velocity estimation is possible when combined with a simple filter. Also, the computational burden of the angular velocity estimator combined with a simple filter is far less than a Kalman filter, but a Kalman filter using a complete dynamics model might produce even more accurate results.

Acknowledgments

The author thanks F. Landis Markley and Paul Mason from NASA Goddard Space Flight Center, Greenbelt, Maryland; Puneet Singla from Texas A&M University, College Station, Texas; and several anonymous reviewers for many helpful comments and suggestions.

References

[1] Ju, G., Pollack, T., and Junkins, J. L., "DIGISTAR II Micro-Star Tracker: Autonomous On-Orbit Calibration and Attitude Estimation," American Astronautical Society, AAS Paper 99-431, Aug. 1999.

[2] Shuster, M. D., "A Survey of Attitude Representations," *Journal of the Astronautical Sciences*, Vol. 41, No. 4, 1993, pp. 439–517.

[3] Shuster, M. D., "Maximum Likelihood Estimation of Spacecraft Attitude," *Journal of the Astronautical Sciences*, Vol. 37, No. 1, 1989, pp. 79–88.

[4] Kincaid, D., and Cheney, W., *Numerical Anaylsis*, 2nd ed., Brooks/Cole Publishing Co., Pacific Grove, CA, 1996, Chap. 7.1, p. 513.

[5] Samaan, M. A., Mortari, D., and Junkins, J. L., "Predictive Centroiding for Single and Multiple FOVs Star Trackers," American Astronautical Society, AAS Paper 02-103, Jan. 2002.

[6] Lewis, F. L., *Optimal Estimation with an Introduction to Stochastic Control Theory*, Wiley, New York, 1986, Chap. 2.4, pp. 88–94.